# Appendix S1

*Evaluating the performance of temporal and spatial early warning statistics of algal blooms*

CD Buelo, ML Pace, SR Carpenter, EH Stanley, DA Ortiz, DT Ha

*Ecological Applications*

## Section S1: Quickest Detection Method Details

The Quickest Detection method, also called the Shirayaev-Roberts procedure, is an 'online' method that updates with each newly collected data point. It is based on the Shiryaev-Roberts (S-R) statistic, which accumulates evidence as to whether an event has occurred based on the likelihood ratio of two models (Polunchenko and Tartakovsky 2012). For our purposes, an event corresponds to a shift from a baseline (high resilience) state to an alarm (low resilience) state, with each state defined by a distribution of rolling window early warning statistics (Carpenter et al. 2014). When the S-R statistic crosses a threshold, it triggers an alarm indicating it is likely the event has occurred and the system has changed state. After an alarm is triggered, the S-R statistic resets and is able accumulate more evidence and trigger additional alarms. The alarm response is described in equations 1 - 3:

$$R_t = \begin{cases} (1 + R_{t-1}) * \Lambda_t, \; R_{t-1} < A \\ \Lambda_t, \; R_{t-1} \geq A \end{cases} \qquad \text{(Eq. S1)}$$

$$\Lambda_t = \frac{g(x_t)}{f(x_t)} \qquad \text{(Eq. S2)}$$

$$I_t = \begin{cases} 0, \; R_t < A \\ 1, \; R_t \geq A \end{cases} \qquad \text{(Eq. S3)}$$

where $R_t$ is the Shiryaev-Roberts statistic at time t, $A$ is the alarm threshold, $\Lambda_t$ is the likelihood ratio of the alarm state model *g()* and baseline state model *f()* evaluated at the data point $x_t$, and $I_t$ is an indicator for whether an alarm has been triggered at time t. The alarm threshold $A$ can be set based on the user's tolerance for false alarms assuming the input data meet certain statistical assumptions (Pollak and Tartakovsky 2009); in practice we have found alarm timing to be insensitive across broad ranges of *A* (Carpenter et al. 2014) and use *A* = 10^7 (Wilkinson et al. 2018).

**Baseline and alarm models**

The data points $x_t$ are the EWS time series, rolling window standard deviation (SD) and autocorrelation (AR(1)), observed in the experimental lake. The models for the baseline *f()* and alarm *g()* states are determined by the reference lake EWS and expectations from theory, respectively, and are statistic specific. For both SD and AR(1), the baseline state model *f()* is centered at the observed EWS value in the reference lake to control for variation in EWS not caused by the manipulation in the experimental lake (storms, seasonal trends, etc).

*SD*

For rolling window SD, both *f()* and *g()* are normal distributions:

$$f(x_t) \sim N(\mu_{baseline}, \sigma_{pool}) \qquad \text{(Eq. S4)}$$

$$g(x_t) \sim N\left(\mu_{alarm}, \sigma_{pool}\right) \qquad \text{(Eq. S5)}$$

where $x_t$ is the observed rolling window SD in the experimental lake, $\mu_{baseline}$ is the observed rolling window SD in the reference lake and $\mu_{alarm} = \mu_{baseline} + 2 * \sigma_{pool}$ . $\sigma_{pool}$ is the pooled standard deviation of rolling window SD in both lakes as in Wilkinson et al. 2018 (Supplemental Information):

$$\sigma_{pool} = \sqrt{\sigma_{rw,exp}^2 + \sigma_{rw,ref}^2} \qquad \text{(Eq. S6)}$$

where $\sigma_{rw,exp}$ and $\sigma_{rw,ref}$ are the standard deviations of the observed rolling window standard deviations, $sd_{rw}$ in the experimental and reference lakes, respectively:

$$\sigma_{rw,i} = sd(rolling\ window\ SD_i) = sd(x_{t,i}) = \sqrt{1\frac{1}{4*x_{t,i}^2} * x_{t,i}^4 * (\frac{2}{N-1} + \frac{\kappa}{N})} \quad \text{(Eq. S7)}$$

where $x_t$ is the observed rolling window SD, $N$ is the sample size (rolling window width), and $\kappa$ is sample kurtosis.

*AR(1)*

For rolling window AR(1), we use the exact probability distribution for Pearson sample correlation coefficient:

$$f(r,\rho,N) = \frac{(N-2)*\Gamma(N-1)*(1-\rho^2)^{\left(\frac{N-1}{2}\right)}*(1-r^2)^{\left(\frac{N-4}{2}\right)}}{\sqrt{2\pi}*\Gamma\left(N-\frac{1}{2}\right)*(1-\rho r)^{N-\frac{3}{2}}} * \quad {}_2F_1(\frac{1}{2},\frac{1}{2};\frac{1}{2}(2N-1);\frac{1}{2}(\rho r+1)) \quad \text{(Eq. S8)}$$

where $r$ is the observed (sample) rolling window AR(1) coefficient, $\rho$ is the population correlation coefficient, $N$ is sample size (rolling window width), $\Gamma()$ is the gamma function, and ${}_2F_1()$ is the Gaussian hypergeometric function. Note f(r,ρ,N) in equation 8 refers generically to the probability density function for correlation coefficient and not the baseline state; below the baseline state likelihood model is denoted $f_{baseline}()$ to differentiate:

$$f_{baseline}(x_t) = f(x_t, \rho_{baseline}, N) \quad \text{(Eq. S9)}$$

$$g(x_t) = f(x_t, \rho_{alarm}, N) \quad \text{(Eq. S10)}$$

where $x_t$ is the observed rolling window AR(1) in the experimental lake at time $t$, $\rho_{baseline,t}$ is the observed rolling window AR(1) in the reference lake, and $\rho_{alarm}$ is the “true” correlation coefficient of the alarm state. We use $\rho_{alarm}$ =0.95 based on theoretical expectations that AR(1) should increase towards 1 as a critical transition is approached (Dakos et al. 2012). The above formulation for AR(1) quickest detection alarms differs from previous applications, which used normal distributions for $f()$ and $g()$ with $\mu_{baseline}$ =$x_{t,ref}$ and $\mu_{alarm}$ =1 and either fixed $\sigma$ values (Carpenter et al. 2014) or time-varying $\sigma$ derived from first-order error propagation (Wilkinson et al. 2018). While qualitatively very similar (*$f(x_t)$* centered on the observed autocorrelation in the reference lake, *$g(x_t)$* at/near the theoretical value of 1 at the critical point), the new “exact” formulation presented here represents an improvement as the probability density function of *f()* and *g()* lies entirely within the domain of the Pearson correlation coefficient (-1 to 1) and avoids erroneous alarms that occur when experimental lake AR(1) is less than reference lake AR(1) (see Appendix S1 and Figure S3 of Wilkinson et al. 2018 Supporting Information).

**References**

Polunchenko, A and AG Tartakovsky. 2012. State of the art in sequential change-point detection. Meth. Comput. Appl. Probabil. 14: 649-683.

Carpenter, SR, WA Brock, JJ Cole, ML Pace. 2014. A new approach for rapid detection of nearby threshold in ecosystem time series. Oikos 123(3): 290-297.

Pollak, M and AG Tartakovsky. 2009. Optimality of the Shiryaev-Roberts procedure. Stat. Sin. 19: 1729–1739.

Wilkinson, GM, SR Carpenter, JJ Cole, ML Pace, RD Batt, CD Buelo, JT Kurtzweil. 2018. Early warning signals precede cyanobacterial blooms in multiple whole-lake experiments. Ecol. Monogr. 88(2): 188–203.

Dakos, V, EH van Nes, P D’Odorico, M Scheffer. 2012. Robustness of variance and autocorrelation as indicators of critical slowing down. Ecology 93(2): 264–271

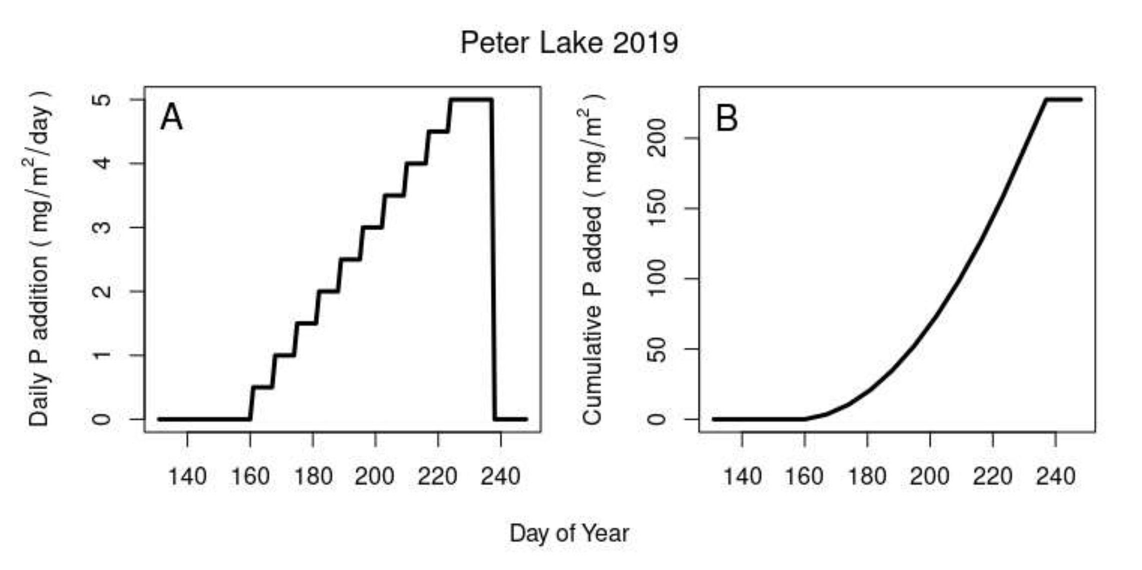


**Figure S1.** Daily (A) and cumulative (B) phosphorus added to Peter Lake in 2019. Nitrogen additions followed the same pattern at 15:1 N:P molar ratio.

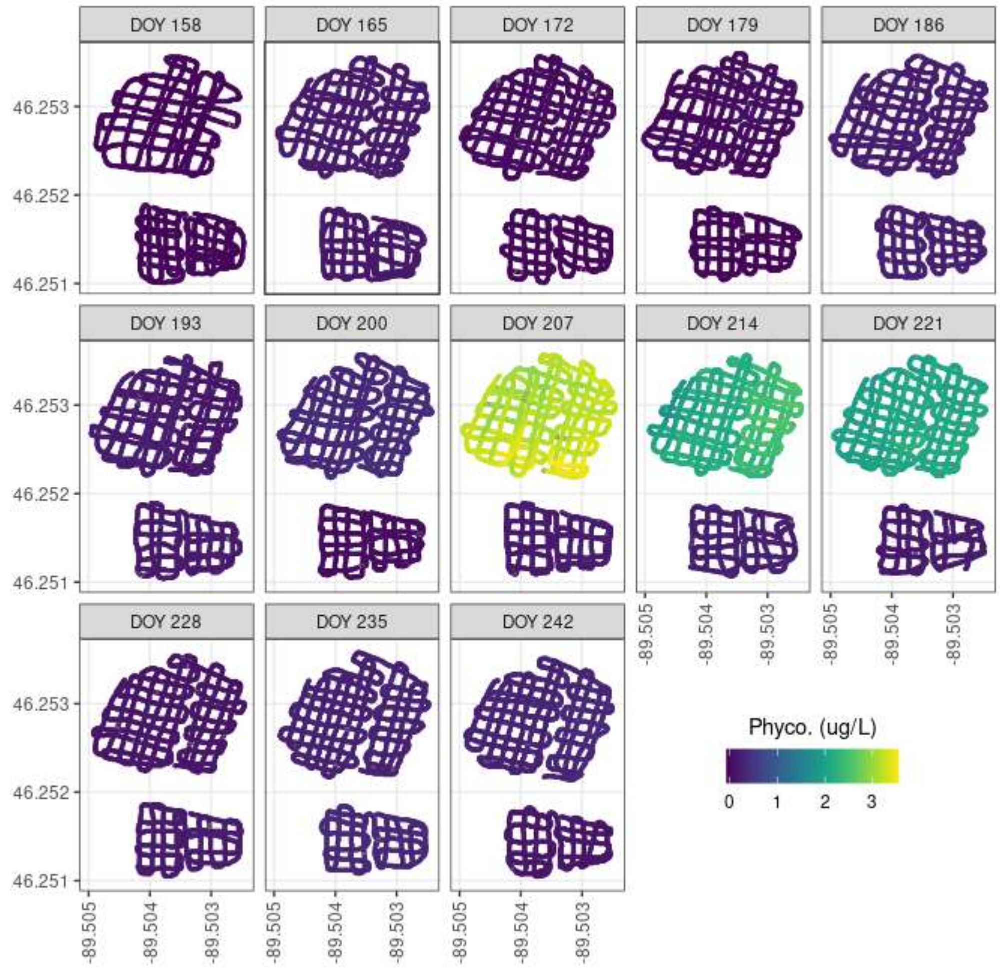


**Figure S2.** Spatial measurements of phycocyanin in Peter (top basin) and Paul (bottom basin) lakes every 7 days in 2019.

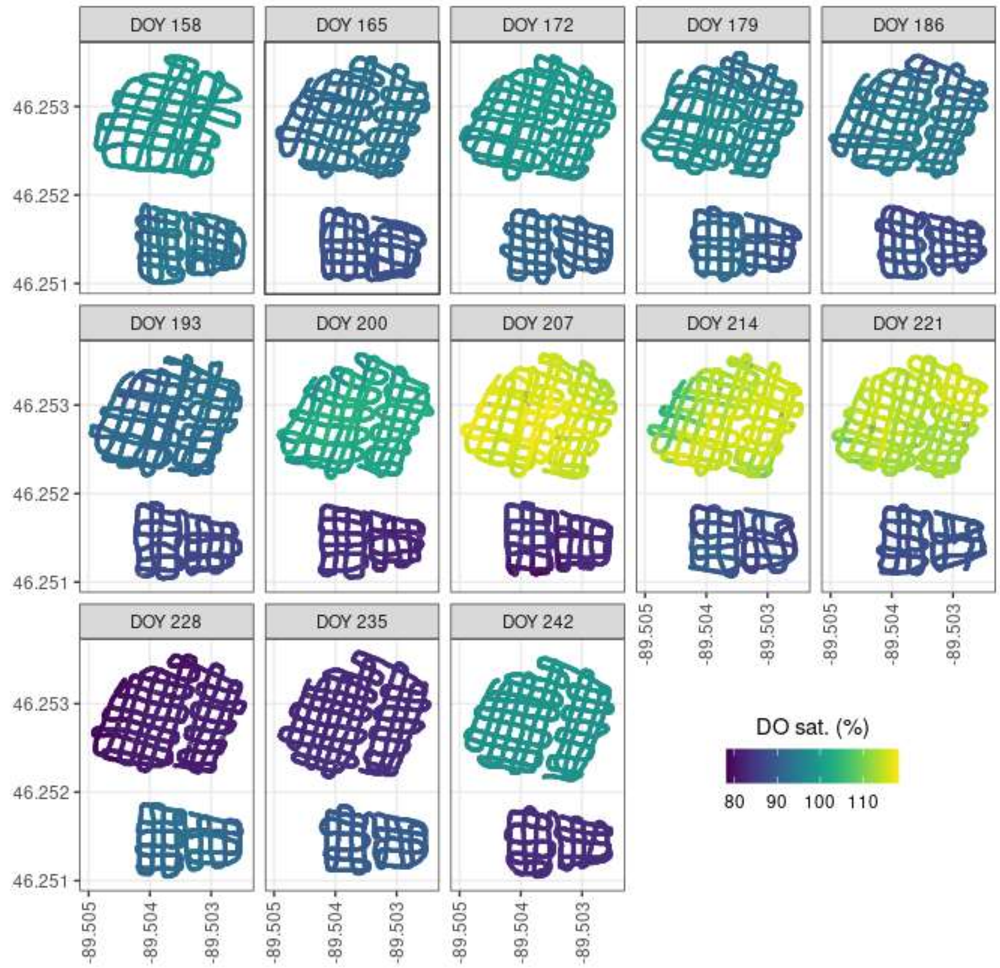


**Figure S3.** Spatial measurements of dissolved oxygen in Peter (top basin) and Paul (bottom basin) lakes every 7 days in 2019.

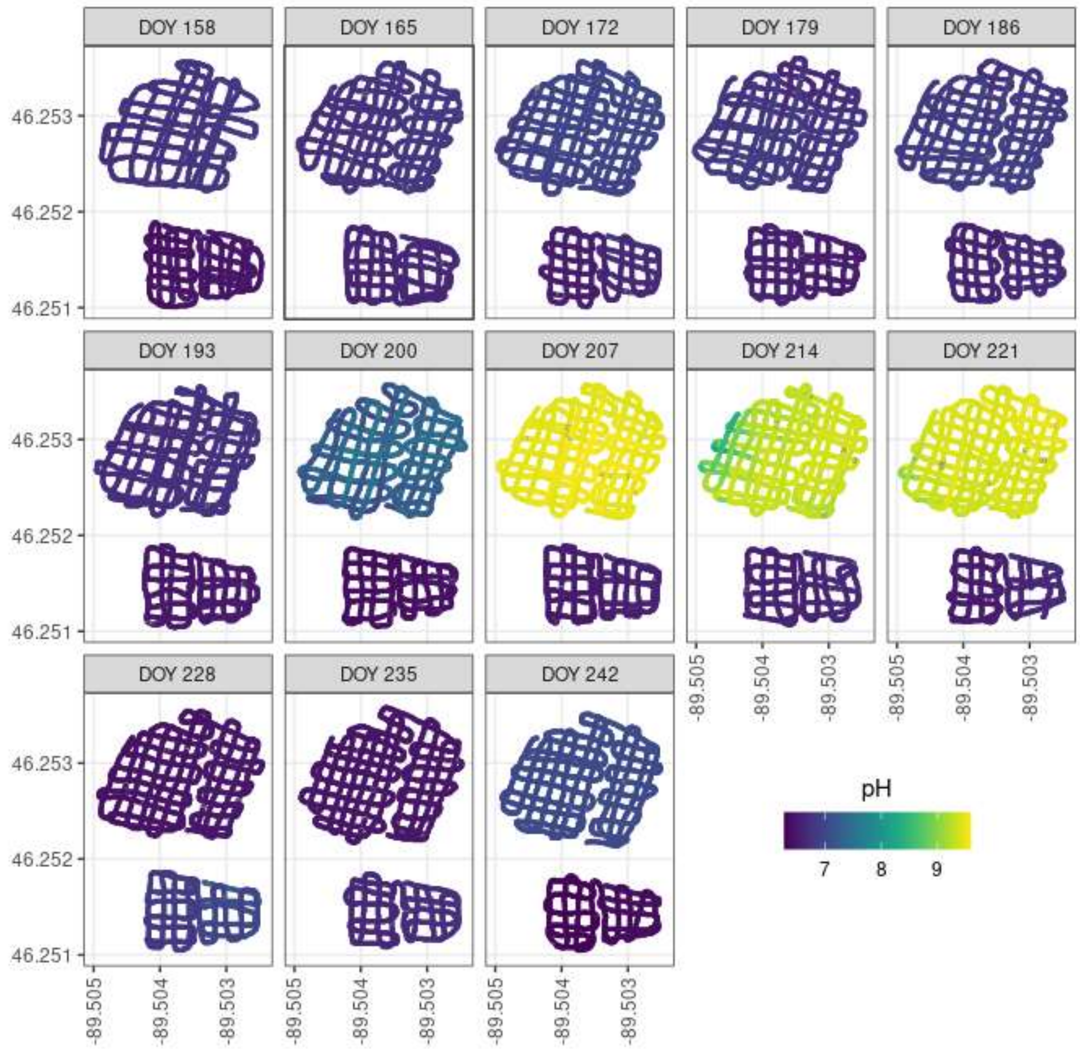


**Figure S4.** Spatial measurements of pH in Peter (top basin) and Paul (bottom basin) lakes every 7 days in 2019.

**Additional EWS: skewness and kurtosis**

<u>Temporal EWS</u>

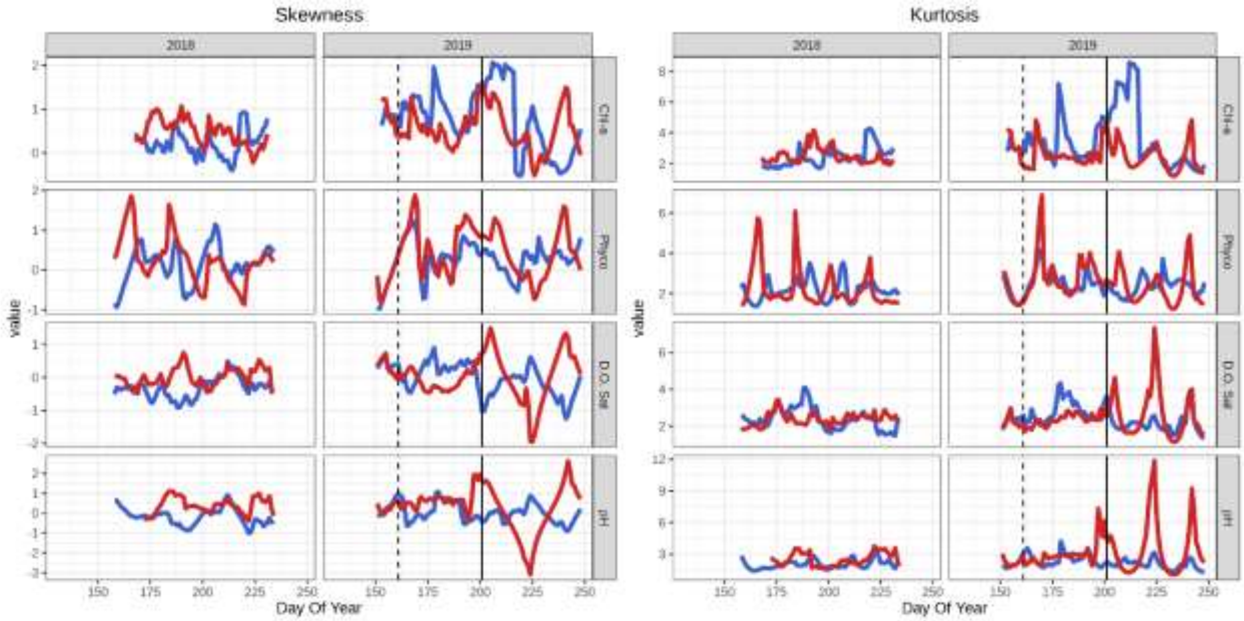


**Figure S5.** Rolling window skewness (left) and kurtosis (right) for Peter Lake (red) and Paul Lake (blue) for 21-day windows. The dashed vertical line is the start of daily nutrient additions and the solid vertical line is when Peter Lake crossed the bloom chlorophyll-a threshold in 2019.

Spatial EWS

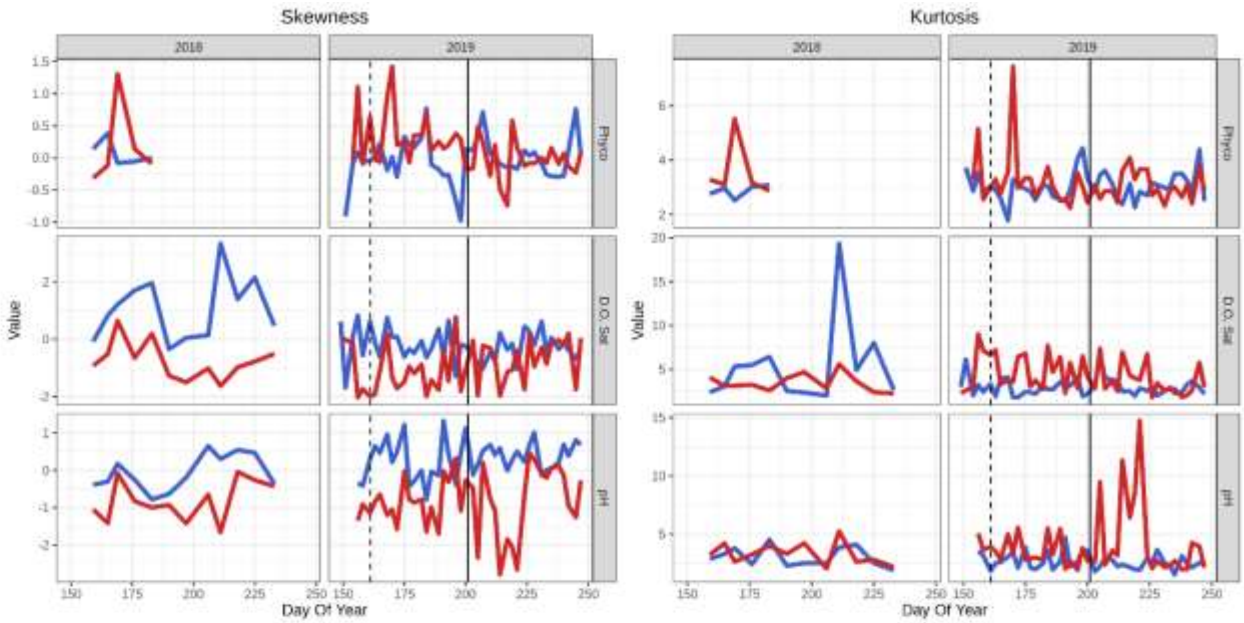


**Figure S6.** Spatial skewness (left) and kurtosis (right) for Peter Lake (red) and Paul Lake (blue). The dashed vertical line is the start of daily nutrient additions and the solid vertical line is when Peter Lake crossed the bloom chlorophyll-a threshold in 2019.

**Table S1.** Summary of differences between lakes and trends during the pre-bloom fertilization period for temporal and spatial skewness and kurtosis.

| | Temporal | | Spatial | | | |
|---|---|---|---|---|---|---|
| | Skewness | Kurtosis | Skewness | | Kurtosis | |
| **Variable** | **Slope** | **Slope** | **Exp. vs. Ref.** | **Slope** | **Exp. vs. Ref.** | **Slope** |
| Chl-a | 0 | 0 | | | | |
| Phyco | 0 | + | ≈ | 0 | ≈ | - |
| DO sat. | 0 | 0 | < | 0 | > | 0 |
| pH | 0 | + | < | 0 | > | 0 |

- Slope denotes if the difference between lakes (experimental lake – reference lake) increased significantly through time (+, $p < 0.05$), decreased (–, $p < 0.05$), or was not significant (0, $p > 0.05$).
- "Exp. vs. Ref." denotes if the mean difference between lakes (experimental lake – reference lake) was positive (>, $p < 0.05$), negative (<, $p < 0.05$), or not significantly different from zero (≈, $p > 0.05$).